Estimation of a Multimass System Using the LWTLS and a Coefficient Diagram for Vibration-Controller Design

Estimation of a Multi-Mass System Using the LWTLS and a Coefficient Diagram for Vibration Controller Design

Y. Yoshioka* and T. Hanamoto**

* Fuji Electric Advanced Technology Co., Ltd., 1, Fuji-machi, Hino-city, Tokyo 191-8502, Japan

** Kyusyu Institute of Technology, 2-4 Hibikino, Wakamatsu-ku, Kitakyusyu 808-0196, Japan

***Abstract*--Vibration caused by a mechanical resonance and time delay caused by signal detection and transmission degrade the control performance of a servo controller for a multi-mass mechanical system. A precise numerical model that represents resonance characteristics and time delay is necessary to design a desired control system. This paper presents an identification method using the iterative process of the linearized and weighted total least squares method. The proposed method derives a transfer function without any prior knowledge of resonance characteristics and time delay. The order of the transfer function is determined with a coefficient diagram that shows coefficients of the denominator of the transfer function. Identification results with an experimental setup are shown to demonstrate the performance of the proposed method. A velocity servo controller with vibration suppression control is designed with the transfer function, and control performance is verified with the experimental setup to validate the transfer function.**

***Index Terms*—multi-mass mechanical system, mechanical resonance, system identification, time delay.**

I. Introduction

Recently, production machinery has employed mechanical components with low rigidity, because the demand for reductions in weight and cost has been increasing. On the other hand, a control system that drives a mechanical system has increasingly required high-response and high-precision servo control performance because of the rising demand for high-speed operation of machinery. However, if the control system drives the mechanical system with low rigidity, vibration caused by a mechanical resonance degrades the control precision. Therefore, it is necessary to optimally design the control system in consideration of mechanical resonant characteristics [1], [2], [3], [4]. In addition, time delay such as signal detection and transmission degrades the control performance as well as the stability of the control system. Accordingly, in order to design a desired control system, a numerical model representing mechanical resonance characteristics and time delay is necessary.

Conventionally, the differential iteration method and the circle curve fitting method have been used as the modal identification method. A numerical model in the form of differential equations is derived. Those methods have recently been applied to the identification of a number of vibration modes over a wide range of frequencies [5], [6]. However, those methods require prior knowledge of vibration modes, such as the number and the distribution of vibration modes of a system to be identified. Moreover, time delay is not considered with those methods.

Recently, several identification methods for a mechanical system have been presented [7]-[11]. Linear least squares method is used to estimate parameters of a model. The global search technique using a genetic algorithm is used to identify parameters of a non-linear mechanical system. Non-linear least squares method is utilized to obtain a model of a mechanical system. However, the structure of the model, such as the number of parameters, is defined preliminarily for those identification methods. The solution of linear least squares method contains bias error caused by the linearization of a transfer function. A genetic algorithm requires the searching process not to trap at local solution. Non-linear least squares method needs initial values of parameters for iterative process. Thus, it follows that those identification methods require prior knowledge of a mechanical system.

Authors have proposed an identification method using the linearized and weighted total least squares method (LWTLS method) in discrete time system [12]. The LWTLS method derives a pulse transfer function with reference to the frequency response data of a multi-mass mechanical system to be controlled, taking account of outliers in a data set. The proposed method adopts the iterative process that eliminates bias error caused by the linearization. Initial values for the iterative process are not required. The pulse transfer function that properly represents mechanical resonant characteristics and time delay is derived without any prior knowledge of a multi-mass mechanical system to be identified. During the identification process, the proper order of the pulse transfer function is determined with the evaluation of the rank of the Sylvester matrix that is composed of coefficients of the pulse transfer function.

Although the derived pulse transfer function can be applied directly to design a digital control system, the transformation from discrete to continuous time is required in order to analyze the resonance frequency and the anti-resonance frequency of the mechanical system. Besides, a continuous time model, such as a transfer

function, is necessary to design parameters of a controller and a compensator in continuous time system directly.

This paper presents an identification method using the LWTLS method for deriving a continuous time model. With the proposed identification method, a transfer function that models mechanical resonant characteristics and time delay can be obtained directly without the process of the transformation from discrete to continuous time. The proposed method also adopts the iterative process that eliminates bias error caused by the linearization. The convergence of iterative process is evaluated simply with the deviation ratios of coefficients of the derived transfer function during the iterative process.

As for the order determination, the evaluation of the rank of the Sylvester matrix requires the extra computation that calculates singular values of the Sylvester matrix during the identification process. In this paper, the order determination using a coefficient diagram is proposed. In the coefficient diagram, the horizontal axis shows the order in linear scale, while vertical axis logarithmically shows coefficients of the denominator of the derived transfer function. The proper order for the transfer function is evaluated with the pattern of the coefficient diagram. If a chosen order is the proper order, a transfer function that properly models both mechanical resonant characteristics and time delay is derived, and the coefficient diagram shows a convex curve. The convexity of the coefficient diagram is utilized to determine whether the chosen order is the proper order. The proposed order determination does not require any statistical analysis using extra data and the calculation of singular values.

In Section II, the configuration of an experimental setup of a multi-mass mechanical system is described to show vibration caused by a mechanical resonance and time delay caused by signal detection and transmission. The significance of the derivation of a numerical model is also indicated. In Section III, the procedure of the LWTLS method to obtain the continuous time model is described, and the application of the coefficient diagram to the order determination is introduced. The proposed identification method has been demonstrated with the experimental setup to show the identification performance. Identification results are shown in Section IV. A derived transfer function has been used to design a velocity controller with vibration suppression control in order to demonstrate the validity of the derived transfer function. Control performance of the velocity controller has been evaluated with the response of the velocity controller to a step change in the velocity reference and the torque reference. Experimental results of velocity control are shown in Section V.

II. Configuration of an Experimental Setup

Fig. 1 shows an experimental setup. TABLE 1 shows the specification of the setup. TABLE 2 shows the specification of the mechanical system. The setup is composed of a three-mass mechanical system, a servo amp, and an external controller. The mechanical system consists of a motor and two disks. The motor and the disks are connected by a thin shaft with low torsional rigidity. Therefore, vibration caused by mechanical resonance between the motor and two disks occurs.

The servo amp drives the motor in accordance with the torque reference signal that is generated from the external controller. The external controller consists of a digital signal processor (DSP), a DA converter, a counter, and an incremental encoder that is Encoder 1 in Fig.1. Encoder 2 is used to only observe the velocity of the shaft edge. Rotational position of the motor shaft is detected with Encoder 1, and electrical pulse signals are transmitted to the counter. The motor velocity is calculated at the DSP with the counter value. The torque reference signal is regulated in accordance with the detected motor velocity and transmitted to the servo amp via the DA converter. The servo amp has an input filter that is the first order lag filter with a time constant of about 1ms. Signal detection and transmission with the encoder, the counter, the DSP, and the DA converter cause time delay. The calculation of the motor velocity in the DSP also causes time delay.

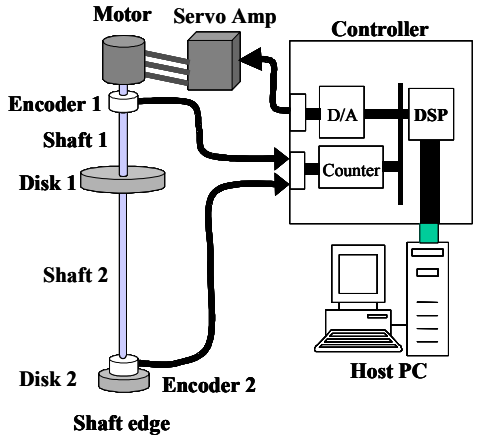

Fig. 1 Experimental setup

TABLE 1
Specification of an Experimental Setup

Rated velocity of motor	[r/min]	3,000
Rated torque	[Nm]	1.27
Resolution of incremental encoder	[p/r]	6,000
Sampling frequency of DSP	[Hz]	4,000

TABLE 2
Specification of a Mechanical System

Number of Mass		3
Inertia [10^{-5}Kgm^2]	Motor	3.54
	Disk 1	13.2
	Disk 2	8.79
Spring constant [Nm/rad]	Shaft 1	64.3
	Shaft 2	29.8

Time delay among the encoder, the DSP, and the DA converter is assumed to be four sampling periods.

Accordingly, in order to design a desired controller installed in the DSP, it is necessary to take account of mechanical resonance and time delay.

III. Identification Method

A. Procedure of the LWTLS Method

Fig. 2 shows the whole identification process to obtain a numerical model of a multi-mass mechanical system.

The first stage is the collection of sampled input-output data from a system to be identified. For the identification of the multi-mass mechanical system to be controlled, torque reference signal, which is the pseudo-random binary signal [10], is generated from the DSP as input signal. The motor velocity that is the response of the torque reference signal is measured at the DSP as output signal for the identification.

In the second stage, frequency response data are obtained with the multi-decimation identification method using the sampled input-output data [5], [13].

After obtaining frequency response data, in the third stage, the iterative process of the LWTLS method is applied to derive a transfer function with reference to a set of the frequency response data. The derived transfer function models overall characteristics combining the mechanical resonance characteristics, phase lag, and time delay. Accordingly, the derived transfer function is suitable for designing a controller installed in the DSP.

The LWTLS method in the third stage is a methodology of deriving the transfer function that is linked by relation as in (1).

$$G(s_k) \approx \left(b_0 + \sum_{i=1}^{r} b_i {s_k}^i \right) \Big/ \left(1 + \sum_{i=1}^{r} a_i {s_k}^i \right) \tag{1}$$

where $G(s_k)$ is the frequency response data, a_i, b_i are coefficients, r denotes the order. s_k is a complex variable defined by (2).

$$s_k = j2\pi f_k \tag{2}$$

where j is the imaginary unit, and f_k is the k_{th} frequency point within the frequency range to be identified.

In order to avoid the nonlinear least squares solution that requires the sensitive initial value setting and the evaluation of a convergence to the local solution, the proposed identification method adopts the linearization.

Linearization is to reformulate the equation (1) into a linear equation as in (3) by multiplying the both sides of the equation (1) by the denominator of a transfer function, which constructs the right side of the equation (1).

$$G(s_k) \approx b_0 + \sum_{i=1}^{r} b_i {s_k}^i - G(s_k) \sum_{i=1}^{r} a_i {s_k}^i \tag{3}$$

The discrepancy between the left side and the right side of the equation (3) is not the same as that of the equation (1) as shown in (4). This error is the bias error caused by the linearization.

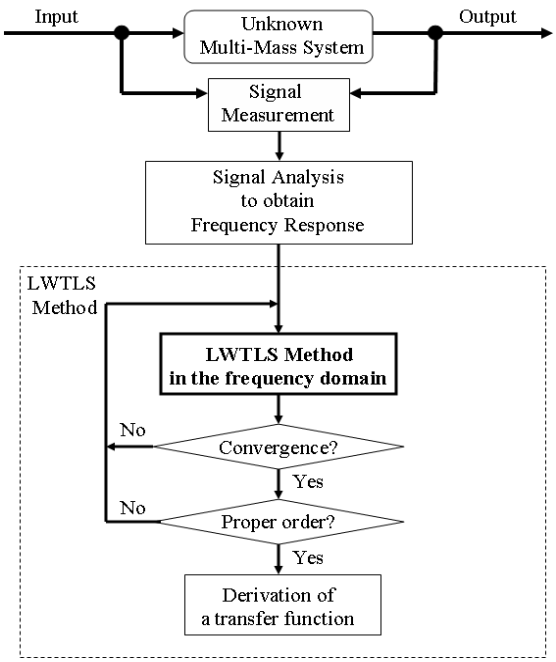

Fig. 2 Procedure of the LWTLS Method

$$E(s_k) \neq \left(1 + \sum_{i=1}^{r} a_i {s_k}^i \right) e(s_k) \tag{4}$$

where $E(s_k)$ is the discrepancy between the left side and the right side of the equation (3) as in (5), $e(s_k)$ is the discrepancy between the left side and the right side of the equation (1) as in (6).

$$E(s_k) = G(s_k) - \left(b_0 + \sum_{i=1}^{r} b_i {s_k}^i - G(s_k) \sum_{i=1}^{r} a_i {s_k}^i \right) \tag{5}$$

$$e(s_k) = G(s_k) - \left(b_0 + \sum_{i=1}^{r} b_i {s_k}^i \right) \Big/ \left(1 + \sum_{i=1}^{r} a_i {s_k}^i \right) \tag{6}$$

In order to eliminate the bias error caused by the linearization, the proposed identification method adopts the iterative process [14], [15]. The procedure of the iterative process of the LWTLS method is described in detail below.

First, the order is set for the equation (3). Next, a complex matrix equation in terms of the coefficients is formulated by constructing a data matrix with the right side of (3) and an observation vector with the left side of (3). In order to eliminate bias error caused by the linearization, a matrix equation as in (7) is formulated with a weighting coefficients matrix that is updated during the iterative process.

$$\mathbf{W}^{(t)}\mathbf{d} \approx \mathbf{W}^{(t)}\mathbf{A}\mathbf{x} \tag{7}$$

where $\mathbf{d}$ is the observation vector, $\mathbf{A}$ is the data matrix, $\mathbf{x}$ is an unknown vector that consists of the coefficients of the transfer function (1), and $\mathbf{W}^{(t)}$ is a diagonal matrix

that consists of weighting coefficients at the t_{th} iteration.

Initial value of the weighting coefficients is set to 1. During the iterative process, the weighting coefficients are set to the reciprocal of frequency response of the numerator derived at the previous iteration as shown in (8).

$$\mathbf{W}^{(t)} = diag({w_1}^{(t-1)}, \mathrm{K}\ , {w_k}^{(t-1)}) \tag{8}$$

where

$${w_k}^{(t)} = 1 \Big/ \left({b_0}^{(t)} + \sum_{i=1}^{r} {b_i}^{(t)} {s_k}^i \right).$$

Conventionally, the ordinary least squares (OLS) method has been used to obtain the solution of (7). The OLS problem seeks to minimize (9).

$$\min \left\| \mathbf{W}^{(t)}\mathbf{d} - \mathbf{W}^{(t)}\mathbf{A}\mathbf{x} \right\|_2 \tag{9}$$

The assumption of the OLS problem is that errors only are included in the observation vector and that errors are not included in the data matrix. This assumption is not correct to obtain the solution of (7), because the data matrix also consists of the frequency data that are affected with measurement errors and calculation errors. The total least squares method is a method that is appropriate to solve (7) when both the observation vector and the data matrix contain errors [16]. The TLS problem seeks to minimize (10).

$$\min \left\| \left[\mathbf{W}^{(t)}\mathbf{A}; \mathbf{W}^{(t)}\mathbf{d} \right] - \left[\mathbf{W}^{(t)}\hat{\mathbf{A}}; \mathbf{W}^{(t)}\hat{\mathbf{d}} \right] \right\|_F \tag{10}$$

where $\|\cdot\|_F$ is the Frobenius norm. Any solution satisfying (11) is called a total least squares solution.

$$\mathbf{W}^{(t)}\hat{\mathbf{d}} = \mathbf{W}^{(t)}\hat{\mathbf{A}}\mathbf{x} \tag{11}$$

In order to take account of the outliers included in the data matrix and the observation vector, the proposed identification method adopts the TLS method to obtain the solution of (7). However, the equation (7) is the complex matrix equation. The equation (7) is reformulated into linear algebraic equations with a diagonal matrix as shown in (12). The diagonal matrix scales the columns of the weighted data matrix. The column scaling is added to obtain the convergence solution of the iterative process.

$$\begin{bmatrix} \mathrm{Re}(\mathbf{W}^{(t)}\mathbf{d}) \\ \mathrm{Im}(\mathbf{W}^{(t)}\mathbf{d}) \end{bmatrix} \approx \begin{bmatrix} \mathrm{Re}(\mathbf{W}^{(t)}\mathbf{A}) \\ \mathrm{Im}(\mathbf{W}^{(t)}\mathbf{A}) \end{bmatrix} \mathbf{M}^{(t)} \left(\mathbf{M}^{(t)} \right)^{-1} \mathbf{x} \tag{12}$$

where $\mathrm{Re}(\cdot)$ indicates the real part of the complex matrix or vector, $\mathrm{Im}(\cdot)$ indicates the imaginary part of those, and $\mathbf{M}^{(t)}$ is the diagonal matrix defined by (13).

$$\mathbf{M}^{(t)} = diag\left\{ 1 / \max\left(\left| \mathbf{v}_i^{(t)} \right| \right) \right\} \tag{13}$$

where $\mathbf{v}_i^{(t)}$ is the i_{th} column vector of the noncomplex data matrix of (12) at the t_{th} iteration, and $\max(\cdot)$ indicates the largest element.

The TLS problem shown in (10) can be solved using the singular value decomposition [17]. The solution of (12) is used to update the weighting coefficients matrix (8) for the next iteration. During the iterative process, the solution of (12), which is coefficients of the derived transfer function, is improved with the weighting coefficients updated.

The convergence of the iterative process is evaluated with the deviation ratios of the coefficients of the derived transfer function as in (14).

$$\begin{aligned} E_a &= \left\{ \sum_{i=1}^{r} \left| \left({a_i}^{(t)} - {a_i}^{(t-1)} \right) \Big/ {a_i}^{(t)} \right| \right\} \Big/ r \\ E_b &= \left\{ \sum_{i=0}^{r} \left| \left({b_i}^{(t)} - {b_i}^{(t-1)} \right) \Big/ {b_i}^{(t)} \right| \right\} \Big/ (r+1) \end{aligned} \tag{14}$$

When either deviation ratios E_a or E_b is smaller than set values, it is supposed that the convergence solution is derived, and the iterative process is interrupted. For an experiment using the setup shown in Fig. 1, the set values are set to 10^{-6}, because the significant digit of the measured input and output data is the millionth digit. The order is evaluated with the proposed order determination using a coefficient diagram. If the chosen order is determined as the proper order, the iterative process finishes. If not, the weighting coefficients in (8) are set to 1, and the process of the LWTLS method is restarted with the different order.

B. Order Determination using a Coefficient Diagram

Conventionally, a coefficient diagram has been used to design a controller for a feedback control system. This design method is called the Coefficient Diagram Method (CDM) [18], [19]. The coefficient diagram is a single logarithmic diagram that shows the coefficients of characteristic polynomial of the feedback control system in logarithmic scale. The coefficient diagram indicates stability, robustness, and control response of the feedback control system. For example, the degree of convexity gives a measure for stability, while the general inclination of the curve gives a measure for the control response. It follows that the specific characteristics of the system give a unique pattern in the coefficient diagram. Therefore, the CDM is used to specify the coefficients of the given controller polynomials in order to obtain the desired characteristics of the feedback control system.

The proposed application of a coefficient diagram is similar to the CDM. However, unlike the CDM, a coefficient diagram is used to determine the proper order for a transfer function, not set the coefficients of the transfer function to obtain the desired characteristics of the transfer function. In the coefficient diagram for order determination, the horizontal axis shows the order in linear scale, while vertical axis shows coefficients of the denominator of the derived transfer function in

logarithmic scale. The transfer function is normalized for the sampling frequency of a control system. It is assumed that the sampling frequency is higher than resonant frequencies. Like the CDM, the specific characteristics of the transfer function give a unique pattern in the coefficient diagram. For example, a transfer function that represents resonant characteristics of the three-mass mechanical system indicates a saw-tooth wave pattern in the coefficient diagram as shown in Fig. 3. In addition, a transfer function that has time delay shows a convex curve in the coefficient diagram irrespective of the order. In Fig. 4, as an example, the upper figure shows a coefficient diagram of the 2_{nd} order transfer function that models time delay for three sampling periods with the Padé approximation formulas, and the lower figure shows the 5_{th} order one.

As described in Section II, the multi-mass mechanical system to be identified is observed from a controller, and the controller is supposed to have time delay such as measurement delay of detectors and transfer delay of control reference signal. Consequently, the derived transfer function has the characteristics of both mechanical resonance and time delay. Therefore, convexity is shown with a saw-tooth wave in the coefficient diagram of the derived transfer function as depicted in Fig. 5. The convexity means that the coefficient diagram shows a convex curve and that a coefficient of the maximum order is not the largest value. Fig. 5 shows a coefficient diagram of a transfer function that represents the characteristics of both mechanical resonance and time delay. The upper figure shows a coefficient diagram when time delay is modeled with the 2_{nd} order transfer function, and the lower figure when time delay is modeled with the 5_{th} order transfer function.

In the identification process, the coefficients of the transfer function for each order are obtained with the order of the transfer function increased. When the order is deficient, the derived transfer function tends to represent only the mechanical resonant characteristics, especially resonance frequency. As the order becomes high, the derived transfer function gradually represents anti-resonance frequency as well as resonance frequency. Then, the derived transfer function represents both time delay and mechanical resonant characteristics when the chosen order becomes sufficiently high. As for the coefficient diagram, a saw-tooth wave pattern is shown when the chosen order is deficient, and a saw-tooth wave pattern turns into a convex curve when the chosen order is sufficient.

The phenomenon described above is used to determine the order for the derived transfer function. The validity of the proposed order determination and the identification performance has been demonstrated with the experimental setup. Identification results are described in the next section.

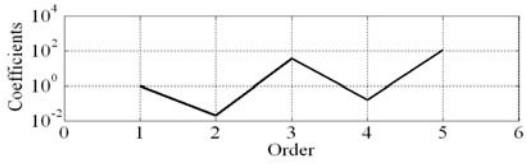

Fig.3 Coefficient diagram indicating resonant characteristics

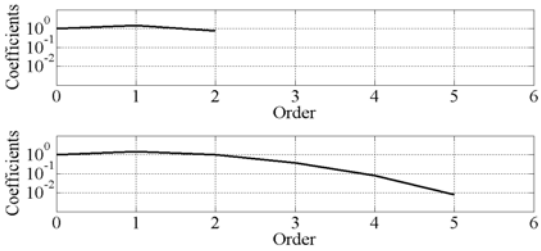

Fig.4 Coefficient diagram indicating time delay

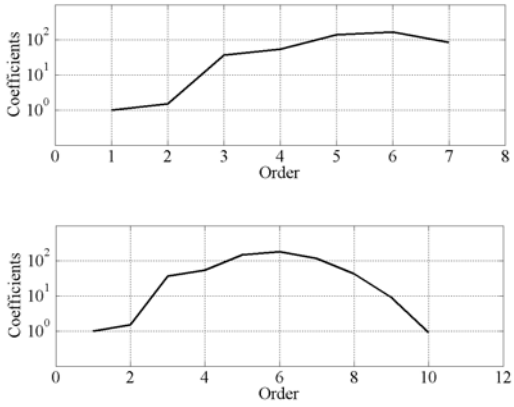

Fig.5 Coefficient diagram indicating resonant characteristics and time delay

IV. Identification Results

First, the three-mass mechanical system shown in Fig. 1 is identified with the 7_{th} order transfer function. Fig. 6-(a) shows a coefficient diagram of the 7_{th} order transfer function. The coefficient diagram shows a saw-tooth pattern. According to the phenomenon described in the previous section, it follows that the coefficient diagram indicates that the chosen order is deficient. Fig. 6-(b) shows the Bode diagram of the 7_{th} transfer function with the heavy line and the measured frequency response with the dotted line. In Fig. 6-(b), normalized frequency is frequency that is normalized to the sampling frequency of the DSP, 4,000Hz, and frequency response below one-fifth of the sampling frequency is shown. As can be seen in Fig. 6-(b), it is confirmed that the 7_{th} order transfer function does not accurately model the three-mass resonant characteristics and phase-lag. It is confirmed that the indication of coefficient diagram is correct.

Next, the three-mass mechanical system shown in Fig. 1 is identified with the 8_{th} order transfer function. Fig. 7-(a) shows a coefficient diagram of the 8_{th} order transfer function. The coefficient diagram shows the convex curve. According to the phenomenon described in the

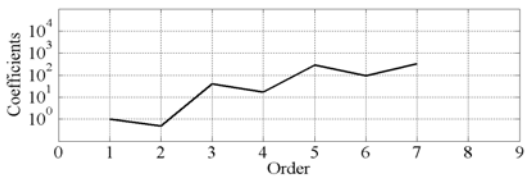

(a) Coefficient diagram

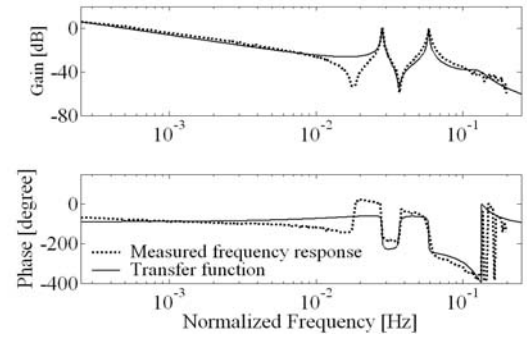

(b) Bode diagram

Fig.6 The 7_{th} order transfer function modeling the three-mass mechanical system

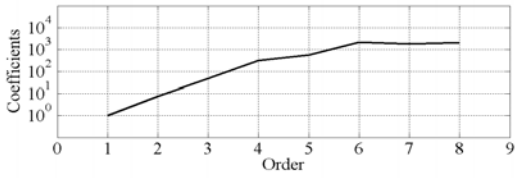

(a) Coefficient diagram

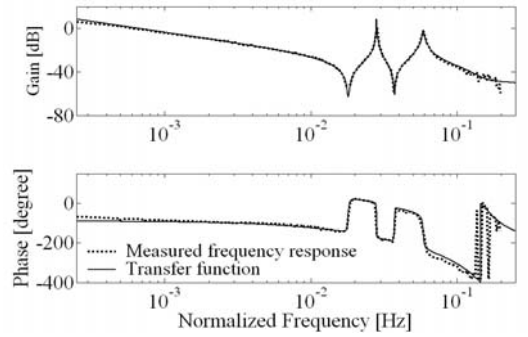

(b) Bode diagram

Fig. 7 The 8_{th} order transfer function modeling the three-mass mechanical system

previous section, it follows that the coefficient diagram indicates that the chosen order is the proper order. Fig. 7-(b) shows the Bode diagram of the transfer function with the heavy line and the measured frequency response with the dotted line. Fig. 7-(b) depicts that the resonant characteristics and phase-lag of the transfer function are almost identical to the measured frequency response. This result shows that the indication of coefficient diagram is correct.

Fig. 8 shows coefficient diagrams when the order is set from 6 to 10. When the order is set to 6, a coefficient of the maximum order, that is the sixth order, is negative value. Therefore, the coefficient of the sixth order cannot be observed in the single logarithmic diagram. As described in the previous section, it can be seen that a saw-tooth wave pattern turns into a convex curve as the order becomes high. When the order is set to higher than 8, a convex curve is shown in the coefficient diagram. The purpose of the identification is to derive the minimal order transfer function that represents the characteristics of both mechanical resonance and time delay. Therefore, it follows from the identification results shown in Fig. 8 that the 8_{th}order is the proper order.

V. Validation of the Derived Transfer Function

A. Model Analysis

First, the chosen order is verified. Theoretical order of the three-mass mechanical system is fifth. Time delay is assumed to be modeled with the 2_{nd} order transfer function with the Padé approximation formulas. The servo amp has the first order lag filter. Consequently, the number of the total sum of the evaluated order is 8. Therefore, it is confirmed that the 8_{th} order that is the estimated order with the proposed order determination is the appropriate order.

Next, the identified mechanical resonant characteristics are verified. Estimated resonance

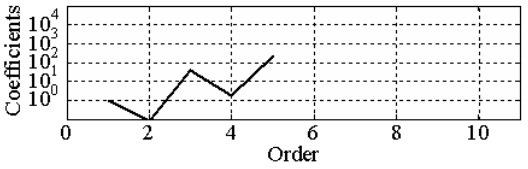

(a) 6_{th} order

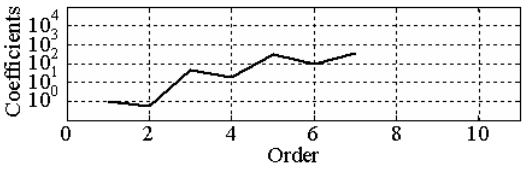

(b) 7_{th} order

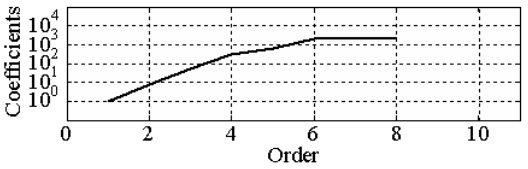

(c) 8_{th} order

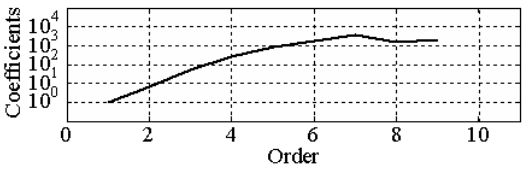

(d) 9_{th} order

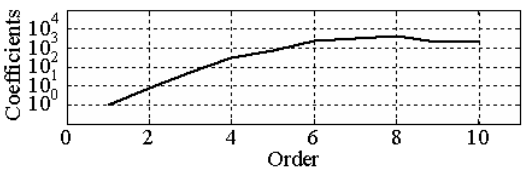

(e) 10_{th} order

Fig. 8 Coefficient diagrams when the order is set from 6 to 10 for the identification of the three-mass mechanical system

frequency and anti-resonance frequency of the three-mass mechanical system are shown in TABLE 3. Those values are obtained by analyzing the roots of the numerator and the denominator of the 8_{th} order transfer function. Theoretical resonance frequency and anti-resonance frequency calculated by using the specification in the TABLE 2 are also shown in TABLE 3. TABLE 3 shows that the relative error between the estimated and theoretical value is less than 5 %. Therefore, it is confirmed that the three-mass mechanical system can be identified sufficiently with the 8_{th} order transfer function.

B. Design of the Velocity Controller

In order to demonstrate the validity of a numerical model, a motor velocity feedback control system is designed by applying the 8_{th} order transfer function that is derived with the proposed identification method. Fig. 9 shows a block diagram of the motor velocity feedback control system. $r(t)$ is a reference of motor velocity, and $y(t)$ is actual motor velocity. $u(t)$ is a torque reference. $N_0(s)/D_0(s)$ is the 8_{th} order transfer function that represents the three-mass mechanical system to be controlled. In order to realize vibration suppression control, feedback compensation [20] is added as a vibration mode compensator. The vibration mode compensator, for example, has been utilized as a damping controller for power system oscillations [21], [22]. The vibration mode compensator is used to shift eigenvalues of the system to be controlled and improve the damping ration of the vibration modes. In order to shift eigenvalues, multiple lead-lag compensators are applied.

Since the main purpose of the controller design is the experimental demonstration of the validity of the derived transfer function, two lead-lag compensators that have the same time constant are used to simplify the design of the time constant. PI controller is used as a feedback controller for simplification. Design procedure for parameters of the vibration mode compensator and PI controller is described blow.

First, parameters of the vibration mode compensator, T_1 and T_2, are designed by means of Bode diagram and the analysis of the poles of the system. In Fig. 10, the thin line shows the frequency response of the vibration mode compensator, and the dotted line shows the frequency response of only the 8_{th} order transfer function. Moreover, the heavy line shows the frequency response of a system that consists of only the 8_{th} order transfer function and the two lead-lag compensators. With reference to the Bode diagram shown in Fig. 10, T_1 and T_2 are selected to increase damping coefficients of two vibration modes of the system that consists of only the 8_{th} order transfer function and the two lead-lag compensators.

Next, a proportional gain K_P and integral gain K_I are adjusted by using computer simulation of the response of the velocity controller to a step change in the velocity reference.

As the design results, TABLE 4 shows the obtained control parameters. TABLE 5 shows damping coefficients of a feedback control system with and without vibration suppression control. For a feedback control system without vibration suppression, the vibration mode compensator is disabled. As shown in TABLE 5, adding the vibration mode compensator increases two damping coefficients.

C. Experimental Results of Velocity Control

Fig. 11 shows experimental results of the response of a feedback control system without vibration suppression control to a step change in the velocity reference. A base

TABLE 3
IDENTIFICATION RESULTS

	Estimated value [Hz]	Theoretical value [Hz]	Relative error [%]
First resonance	234.22	244.81	4.3
First anti-resonance	149.39	147.58	1.2
Second resonance	112.77	112.93	0.1
Second anti-resonance	71.23	69.76	2.2

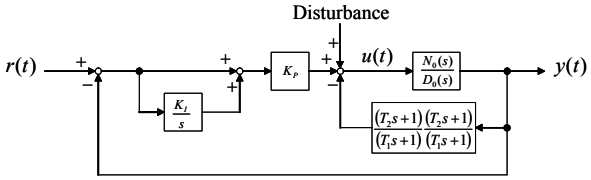

Fig. 9 Motor velocity feedback control system

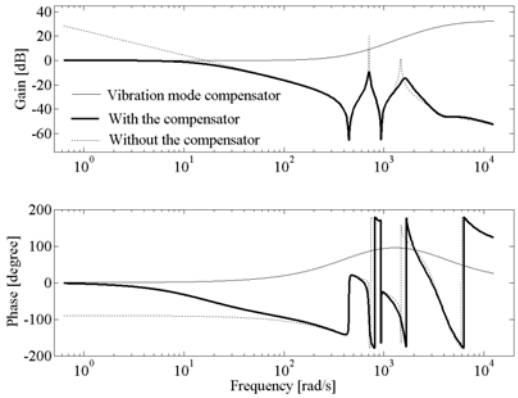

Fig. 10 Bode diagram for controller design

TABLE 4
CONTROL PARAMETERS

	With Vibration suppression	Without Vibration suppression
K_P	1.1	0.5
K_I	18	1
T_1	0.0003	N/A
T_2	0.002	N/A

TABLE 5
DAMPING COEFFICIENTS OF VIBRATION MODES

Vibration mode	With Vibration suppression	Without Vibration suppression
First	0.013	0.0001
Second	0.056	0.002

quantity of per unit value is set to the rated velocity of the motor. The proportional gain cannot be increased because the feedback control system becomes unstable. It can be seen that motor velocity vibrates and edge velocity slightly vibrates.

Fig. 12 shows experimental results of the step responses of a feedback control system with vibration suppression control. Since the stability of the feedback control system increases because of the vibration suppression compensator, the proportional gain can be increased. Therefore, vibration is not only suppressed but also the response of the feedback control system is improved. Vibration of motor and edge velocity is rapidly damped.

Fig. 13 depicts the response to a step change in the torque reference that is added as shown in Fig. 9. The step change is assumed to be the simulated disturbance. Velocity of the motor and the edge are stabilized promptly at reference velocity.

VI. Conclusions

In this paper, an identification method using the iterative process of the linearized and weighted total least squares method has been proposed, and the order determination using the Coefficient Diagram Method has been introduced.

Identification of a three-mass mechanical system using an experimental setup has been carried out. Experimental results demonstrate that a transfer function representing mechanical resonant characteristics and time delay is derived without any prior knowledge of a multi-mass mechanical system, and show that high precision of identification with the proposed method can be realized.

Control system design using a numerical model has been carried out to demonstrate the validity of the proposed identification method. Experimental results of velocity control shows that vibration suppression control can be realized with a vibration mode compensator designed using the numerical model.

Those experimental results demonstrate that the proposed identification method is the promising method.

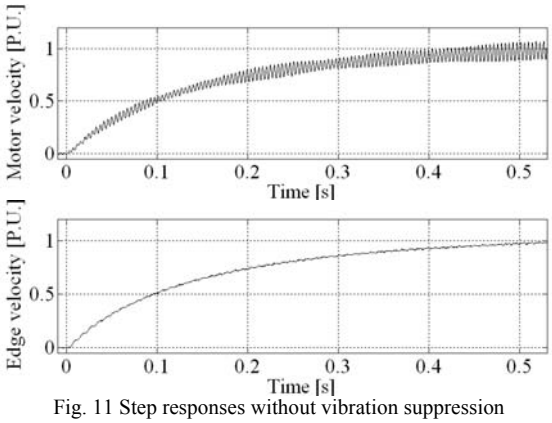

Fig. 11 Step responses without vibration suppression

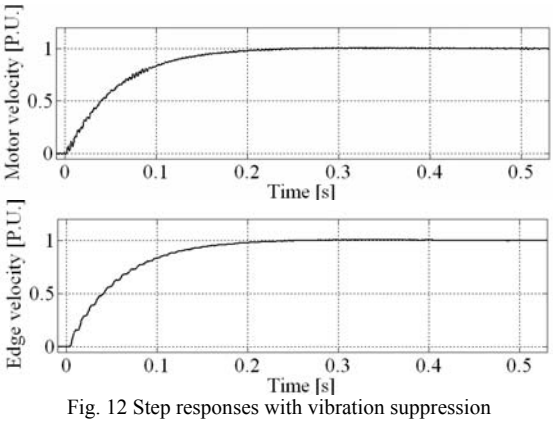

Fig. 12 Step responses with vibration suppression

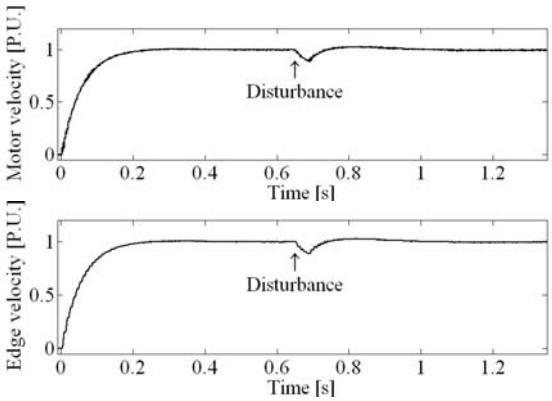

Fig. 13 Disturbance response with vibration suppression

References

[1] N. Matsui, Y. Hori: "Advanced Technology in Motor Control", *T.IEE Japan*, Vol.113-D, No.10, pp.1122-1137, Oct. 1993 (in Japanese).

[2] H. Kobayashi, Y. Nakayama, and K. Fujikawa: "Speed Control of Multi-Inertia System only by a PID Controller", *T.IEE Japan*, Vol.122-D, No.3, pp.260-265, March 2002 (in Japanese).

[3] M. Hosaka and T. Murakami: "Vibration Control of Flexible Arm by Multiple Observer Structure", *Electrical Engineering in Japan*, Vol. 154, No.2, pp. 68-75 2006.

[4] K. Szabat and T. Orlowska-Kowalska: "Vibration Suppression in a Two-Mass Drive System Using PI Speed Controller and Additional Feedbacks-Comparative Study", *IEEE Trans. on Industrial Electronics*, Vol. 54, No.2, pp. 1193-1206, Apr. 2007.

[5] S. Hashimoto, T. Ishikawa, S. Adachi, H. Funato, K. Kamiyama, and A. Isojima: "Multi-Decimation Identification-Based Modeling Method of Flexible Structures for Robust Vibration Control", *T.IEE Japan*, Vol.124-D, No.5, pp.471-478, May 2004 (in Japanese).

[6] M. Iwasaki, M. Kawafuku, and H. Hirai: "Precise Modeling for Mechatronic Systems Using Differential Iteration Method", in *Proceedings of The 2005 International Power Electronics Conference (IPEC-Niigata 2005)*, pp.1575-1579, 2005.

[7] İ. Eker and M. Vural: "Experimental On-Line Identification of a Three-Mass Mechanical system",

[8] I. Z. Mat Darus, F. M. Aldebrez and M. O. Tokhi: "Parametric Modeling of a Twin Rotor System Using Genetic Algorithm", *Proceedings of First International Symposium on Control, Communications and Signal Processing*, pp. 115-118, 2004.

[9] Z.-Y. Yang and T. Hung: "Parameter Identification and Tuning of the Servo System of a 3-HSS Parallel Kinematic

Machine", Int, J. Adv. Manuf. Technol., Vol. 31, pp. 621-628, 2006.
[10] M. Pacas, S Villwock, and T. Eutebach: "Identification of the Mechanical System of a Drive in the Frequency Domain", *Proceedings of the 30th Annual Conference of the IEEE Industrial Electronic Society*, pp. 1166-1171, Nov. 2004.
[11] G. Jin, M. K. Sain, and B. F. Spencer, Jr: "Frequency Domain System Identification for Controlled Civil Engineering Structures", *IEEE Trans. on Control Systems Technology*, Vol. 13, No. 6, pp. 1055-1062, Nov. 2005
[12] Y. Yoshioka and T. Hanamoto: "An Identification Method of the Multi-Mass Resonant Characteristics of a Mechanical System", in *Proceedings of The 2005 International Power Electronics Conference (IPEC-Niigata 2005)*, pp.1803-1809, 2005
[13] Y. Yoshioka and T. Hanamoto: "An Identification Method using the Total Least Squares Method for Vibration Modes for Vibration Suppression Control", *T.IEE Japan*, Vol.126-D, No.6, pp.794-803, 2006 (in Japanese).
[14] C. K. Sanathanan, J. Koerner, "Transfer Function Synthesis as a Ratio of Two Complex Polynomials", *IEEE T.Automatic Control*, Vol.8, pp.56-58 , 1963.
[15] T. Noda, M. Takasaki, H. Okamoto, K. Fujibayashi. H. Nishigaito, T. Okada, "Low-Order Linear Model Identification Method of Power System by Frequency-Domain Least-Squares Approximation," *T.IEE Japan*, Vol.121-B, No.1, pp.52-59, 2001.
[16] S. V. Huffel, J. Vandewalle, The Total Least Square Problem Computational Aspects and Analysis, *SIAM* 1991.
[17] G. H. Golub and C. F. Van Loan, Matrix Computation Third Edition, *The Johns Hopkins University Press*, 1996.
[18] S. Manabe: "Coefficient Diagram Method", in *Proceedings 14th IFAC Symposium on Automatic Control in Aerospace*, pp. 199-210, 1998
[19] S. E. Hamamci, M. Koksal: "Robust Control of a DC Motor by Coefficient Diagram Method", *Proceedings of 9th Mediterranean Conference on Control and Automation*, 2001.
[20] J. Van De Vegte, Feedback Control Systems Third Edition. *Englewood Cliffs, NJ: Prentice Hall*, 1994.
[21] M. E. Aboul-Ela, A. A. Salam, J. D. McCally, and A. A. Fouad: "Damping Controller Design for Power System Oscillations Using Global Signals", IEEE Trans. on Power System, Vol. 11, No. 2, pp. 767-773, May 1996.
[22] R. Sadikovic, P. Korba, and G. Andersson: "Application of FACTS Devices for Damping of Power System Oscillations", *IEEE Power Tech St. Petersburg, Russia*, 2005.